Decision Making and Perceptual Bistability in Spike-Based Neuromorphic VLSI Systems

Federico Corradi*, Hongzhi You†, Massimiliano Giulioni‡, and Giacomo Indiveri*

*Institute of Neuroinformatics, University of Zürich and ETH Zürich, Switzerland
†Key Laboratory for Neuroinformation of Ministry of Education, University of Electronic Science and Technology, China
‡Department of Technologies and Health, Istituto Superiore di Sanità, Roma, Italy

Email: federico@ini.phys.ethz.ch

***Abstract*—Understanding how to reproduce robust and reliable decision making behavior in neuromorphic systems can be useful for developing information processing architectures in subthreshold analog circuits as well as future emerging nano-technologies, that comprise inhomogeneous and unreliable components. To this end, we explore the computational properties of a recurrent neural network, implemented in a custom mixed signal analog/digital neuromorphic chip, for realizing perceptual decision-making, bi-stable perception, and working memory. The chip comprises conductance-based integrate-and-fire neurons and configurable synapses with realistic dynamics. These circuits are configured to implement a recurrent neural network, composed of excitatory and inhibitory pools of silicon neurons coupled with local excitation and global inhibition. We show how the interplay between excitation and inhibition produces competitive winner-take-all dynamics, which is a feature of decision-making and persistent activity models, and demonstrate that the system generates reliable dynamics capable of reproducing both neuro-physiological data and psycho-physical performances in coding and collective distributed computation.**

I. Introduction

Much effort is currently being invested in the quest for developing new computing paradigms for information and communication technologies (ICT): fundamental notions are being revised and fundamental characteristics of new materials are being explored to develop new types of computing systems that can go beyond the Complementary Metal–Oxide–Semiconductor (CMOS) era. In this work we address this challenge by taking inspiration from the efficiency and robustness of neuro-biological systems: we study an implementation of a brain-inspired model of basic computational primitives which uses low-power mixed signal subthreshold analog and asynchronous digital circuits to implement a network of spiking neurons and synapses. Despite the variability and heterogeneity observed in the analog circuits, we demonstrate a reliable neuromorphic implementation of neural processes involved in the foundations of bistable perception, decision making, and working memory.

The ability of embodying information in the dynamics of a recurrent neural network, which can persist also in the absence of external stimulation and transition between meta-stable states, represents a fundamental processing capability of neural systems. We use the framework of recurrent neural networks and meta-stable attractor states to emulate processes that are at the basis of bistable perception, decision making, and working memory. The study of the collective dynamics of multiple neural populations with attractor states has been the subject of a good deal of investigation. This class of network is considered a basic building block for expressing different forms of computation in many different neural systems. In particular, reverberating states of cortical activity are thought to underlie important cognitive processes and functions: it has been shown for example that attractor networks in cerebral cortex are important for long-term memory [1], [2], short-term memory [3]–[5], contextual mental states [6], attention [7], bistable perception [8], [9], and perceptual decision making [10]–[12]. In biological inspired neural network models, it has often been assumed that an attractor in phase space represents an internal or an external source of information [13], [14]. From a biological perspective, recurrent spiking neural network models have expressed the dynamics of bistability in their firing rates. In this work we configured a neuromorphic VLSI chip comprising spiking neurons and dynamic synapses to implement recurrent neural networks with excitatory and inhibitory connections (implementing positive and negative feedback loops respectively). We configured the circuits to implement cortical neural network models and analyzed their dynamics by measuring the neuron's spikes and calculating their mean firing rates.

The paper is organized as follow: in the methods section, we describe the cortical network architecture and its implementation in neuromorphic hardware. In the results section we show how the VLSI network architecture gives rise to bistable dynamics and demonstrate that these network dynamics can reproduce measured psychometric functions in a two choice discrimination task [15]–[17]. In Section IV we discuss the results and present the concluding remarks

II. Materials and Methods

A. Neuromorphic Very Large Scale Integration (VLSI) System

We use an analog/digital mixed signal VLSI neuromorphic device that contains implementations of silicon neurons and synapses using subthreshold analog circuits, and asynchronous memory and communication blocks [18] (see Fig. 1a). Every

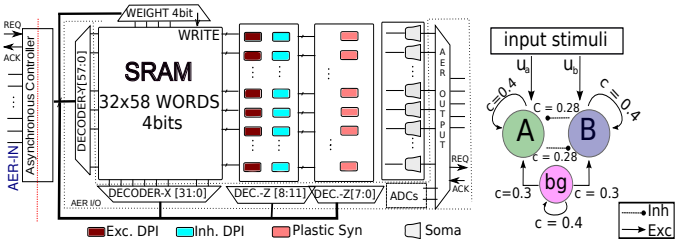

(a) (b)

Fig. 1: a The Neuromorphic VLSI chip, it contains an array of 58 analog integrate-and-fire neurons and programmable synapses implemented with a 4 bit SRAM. b The network consists of three populations of neurons (A, B, bg) recurrently connected. The connectivity in the network is random and sparse. Connectivity levels are as indicated in the diagram.

neuron has 32 programmable synaptic inputs, with synaptic weights stored in 4 bit digital programmable Static Random Access Memory (SRAM) cells. We use the neuromorphic chip interfaced to a standard workstation, via an FPGA board that acts as a mapper [19] to send, receive and route spikes to and from the chip. Additionally the mapper stores the synaptic weight matrix that is used to program the chip's SRAM cells. The neuromorphic chip is also connected to a daughter which is used to configure the analog parameters of the synapses and neurons in the chip. Figure 1a shows the arcturecture of the neuromorphic processor: asynchronous digital events coming from the mapper board are decoded at the input decoder; based on the decoded address the spikes are delivered to one of the excitatory or inhibitory SRAM synapses, or to one of the plastic synapses. The synapses then produce currents with biologically plausible dynamics that are integrated by the neuron. If these integrated inputs are sufficiently large, then the neuron generates a spike that is sent outside via the Address Event Representation (AER) output interface.

The architecture of the network is illustrated in Fig. 1b: it is organized in three populations of neurons, A, B, and background (bg). The number of neurons in population A and B is $N_a = N_b = 22$ while the background population counts $N_{bg} = 12$ neurons. Each population is recurrently connected, with sparse connectivity. Populations A and B inhibit each other via direct inhibitory connections. The connectivity factor c in Fig. 1b refers to the mean number of connections that a neuron makes with other neurons randomly chosen in the target population. The background population provides excitation to populations A and B. We calibrated the architecture parameters such that the two pools of neurons A and B exhibit meta-stable states of activity. The calibration method is based on mean field analysis as described in [20].

III. Results

A. Discrimination of distinct stimuli and basins of attraction

Long-lasting spiking activity in the cortex, that lasts much longer than the typical time scales of synapses and membrane potentials, is the neural correlate of working memory and perceptual decision making. In theoretical neuroscience models this activity is assumed to encode sensory inputs which relate to different alternative possible decisions or percepts [16]. This activity is accumulated in different pools of neurons that, due to their recurrent excitatory connections, are capable of sustaining persistent activity, even after the input stimulus that triggered it is removed. Previous theoretical work has demonstrated that neural circuits of the type shown in Fig. 1b can account for salient characteristics of the neural correlates of perceptual decision making such as psychometric functions and reaction times [16], [17].

We emulated a two choice discrimination task using the two pools of silicon neurons described in Section II-A. In particular, we reproduced the results of a classical neuroscience experiment denoted as the two alternative random moving dots task. In this experiment, monkeys or human subjects have to report the net direction of perceived motion (left or right) of a patch of moving dots on a screen, as a function of the amount of coherently moving dots in one direction, versus the amount of dots moving in random directions. While performing the task, subjects accumulate evidences for a decision and report the perceived direction of motion as quickly as possible. The decision process is triggered when the accumulation of evidence reaches a threshold. The speed of execution of the task depends on the motion coherence (percentage of coherently moving dots in a given direction). In our experiment we bypassed the visual processing stages and stimulated the populations of neurons representing the perception of moving dots directly with computer generated spike trains. In particular, during the stimulation phase, we stimulated both populations A and B with inhomogeneous Poisson spike trains that represent the activity of the middle temporal (MT) visual area during a random moving dots task. In addition, we stimulated all neurons chip with a Poisson spike train of $10\,Hz$ to represent background activity. The mean rates of the input stimuli are expressed as:

$$\begin{aligned} \nu_a^i &= \nu_0 - \alpha \cdot \nu_{coh}^i \\ \nu_b^i &= \nu_0 + \alpha \cdot \nu_{coh}^i \end{aligned} \tag{1}$$

where ν_0 is the base stimulation frequency, α represents a ramping coefficient, ν_{coh}^i represents the percentage of motion coherence, and i indicates the experiment trial. The coherence factor ν_{coh}^i is limited in the range: $0 < \nu_{coh}^i < 100$. Therefore, if ν_{coh} is large, the two populations will receive largely different inputs: ν_a will be large and ν_b will be small. The competition between the two neural populations will eventually collapse in one of the two attractor states. The persistent activity that remains after the input stimulus removal, will be sustained by the recurrent network dynamics. This mnemonic delay period is the neural correlate of working memory. The choice of the network is probed by means of a threshold on the mean firing rates ($\nu_{thr} = 50\,Hz$): when one of the two population exceed this threshold than we assume that the network dynamics has committed to a decision. The time required for the two pools of neurons to finish the competition represents the reaction time of the trial. For trials in which the coherence is equal to zero, the two input stimuli have the same mean frequencies, which indicate a non informative input. While for coherence

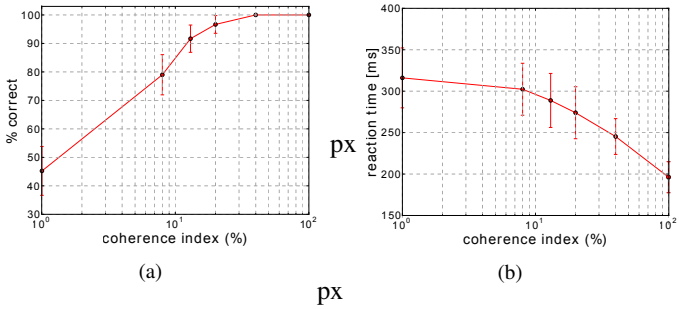

Fig. 2: **Neurometric functions.** Every dot represents the mean of 300 trials. Error bars are the standard deviation. As the coherence level increases the performances increase. Moreover, the reaction time decrease with an increase coherence of the input stimuli which represents an easier discrimination trial.

levels close to 100%, the mean input frequencies are about $\nu_a = 100\,Hz$ and $\nu_b = 0\,Hz$ indicating a complete coherent stimulus.

The decision space can be well represented by a 2D plot in the frequency space ν_a, ν_b. Such a figure describes the time spent by the two populations of neurons at different firing rate frequencies. In Fig. 3 we show three different cases in which the input stimulus was at different coherence levels. On the x-axis we plot the mean firing rate frequency for population A, and on the y-axis we plot the firing rate for population B. Every plot in Fig. 3a, 3c, 3e is the average over 300 trials. At the beginning of the trial, the network dynamics is slowly moved from the spontaneous activity state ($\nu_a \sim \nu_b \sim 5\,Hz$) to a point in which both populations are firing at higher rate. In this phase, the rate of the two populations strictly depends on the input stimuli and the network is integrating evidences for the subsequent decision. After 200 ms from the presentation of the stimulus, the input is removed from the network and the network dynamics collapses in one of the two attractor states A or B. The collapse in one of the two attractor state is the neural correlates of a decision. When the mean firing rate activity is higher for population A (or B) then the network choice is A (or B). In Fig. 3a is shown the decision space for trials in which the coherence level was 0. This means that the network had equal information about the inputs and the choice was made at chance level ($\sim 50\%$). In Fig. 3b ten trials are shown in a mean rates plot. As you can see, after the stimulus removal at 0.2s one of the two population smoothly switches off while the other increases its firing rate. Note that it is not possible to end with both populations firing at elevated reverberant state as the two pools of neurons inhibit each other. Figures 3a, 3b evidence that the choice A and B where almost equiprobable and the network was performing at chance level.

When the coherence of the input stimulus increases the network performs better than chance level. For high coherence of the input, the network is always making the correct decision (see Fig. 2). Figure 2 shows the psychometric functions for six different levels of input coherence. Every dot in the psychometric function is the average over 300 trials. The reaction time indicates the difficulty of the trial. In fact the reaction time decreases for higher coherence of the input

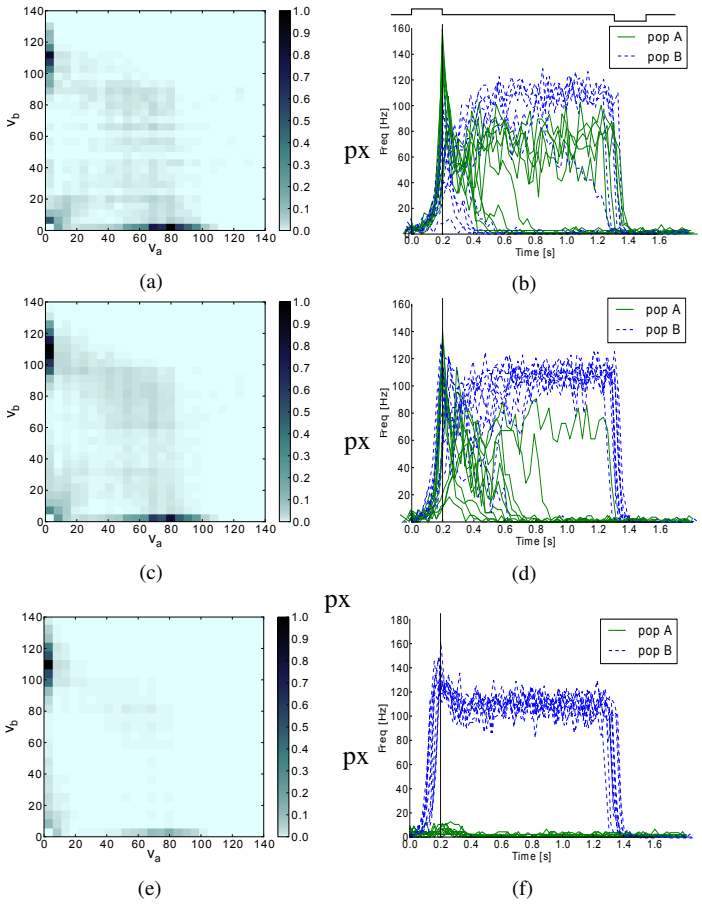

Fig. 3: **Decision space and mean rate plots.** a, b: ν^1_{coh} = 1 %, c, d: ν^2_{coh} = 20 %, and e, f: ν^3_{coh} = 100 %. Plots a, c, e represent the average of 300 trials and they show the averaged network activity, i.e. the mean rate frequency of populations A and B. Figures. b, d, f show the mean firing rates for ten trials for different coherence levels. The square wave at the top of Fig. d indicates that the stimulation phase lasts 200ms and that at 1.4s an inhibitory stimulus is used to suppress reverberant network activity. After the stimulus removal $t = 0.2$, network activity collapses in one of the two attractor states. The density for the A choice decrease as the coherence level for the opposite stimulus increase. This is evident from the smaller blue central blob that gradually decrease in size, from 3a, 3c, to 3e.

stimuli while for low coherence stimuli it saturates around 320 ms, visible in Fig. 2b. The fine tuning of the reaction time can be achieved by driving, with the external input, the system in the proximity of the bifurcation value [17]. This tuning has been exploited in order to achieve biological realistic reaction time as indicated in Fig. 2b.

B. Dynamics of perceptual bistability

When the recurrent connections among neurons that are part of the same population (A, B in Fig. 1b) are strong enough, the network operates in a winner-take-all regime. In this regime, only one excitatory population can be in the attractor state at any point in time. Point-attractor neural networks have two types of stable fixed points of the network dynamics. They exhibit a spontaneous state with a low firing rate (down state), and one or more persistent states with high firing rates in which the activity of the network tends to be stable (attractor or up

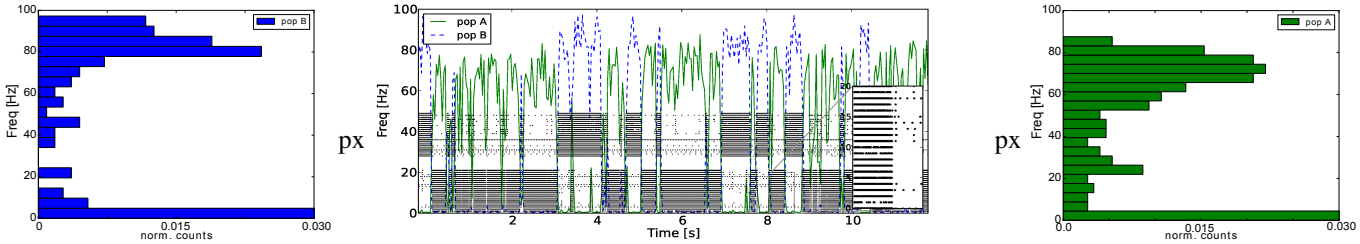

(a) (b) (c)

Fig. 4: **Bistable dynamics.** Populations mean firing rate over time. The input to the network is a constant injection of current in the soma of all neurons.

state). The system will react to external stimulation, i.e. to a destabilizing stimulus, with different patterns of activations but it will always relax toward one of the stable attractor state [21]. In a winner-take-all regime, since the two populations inhibit each other, only one population of neurons can be found in the up state of the network dynamics. The observed behaviour of our neuromorphic attractor network, when all neurons are stimulated by a constant injection of current, is an alternation of perceptual dominance among the two different activity states with very long time constants, orders of seconds. Figure 4 shows five seconds of recordings of such behaviour. The central panel of Fig. 4b, shows the mean firing rate activity over time of neurons grouped in populations. Continuous green line depicts neurons in population A, and the dashed blue line represents neurons in population B. An irregular alternation of high activity is evident, and only one of the two populations of neurons can be found in the up state ($\sim$ 80 Hz) of activity: this is a confirmation that the network is operating in a winner-take-all regime.

IV. Conclusions

We demonstrated an implementation in neuromorphic hardware of basic computational primitives used to produce neural plausible dynamics. In particular, our results well correlate not only with the behavioural responses (the reaction time and the accuracy) of subjects, but also to the neural responses in their cortical areas during a two-choice perceptual discrimination task. Choice formation and successive behaviour coincide with the transition from a spontaneous activity state to the elevated persistent state of activity in a clustered pool of neurons. An important aspect of this work is that reliable computation emerges from simple mismatched analog neurons; mismatch effects are evident in the mean rate plots, of Fig. 4, 1, where the frequency of the up states differ of about 10%.

Acknowledgment

This work has been supported by the European Commission with the "neuroP" Project, ERC-2010-StG-257219-neuroP and by the SiCode EU project, under FET-Open grant number FP7-284553.

References

[1] G. M. Wittenberg, *et al.*, "Synaptic reentry reinforcement based network model for long-term memory consolidation," *Hippocampus*, vol. 12, no. 5, pp. 637–647, 2002.

[2] D. Amit, *Modeling brain function: The world of attractor neural networks*. Cambridge University Press, 1992.

[3] X. Wang, "Synaptic basis of cortical persistent activity: the importance of NMDA receptors to working memory," *Journal of Neuroscience*, vol. 19, pp. 9587–9603, November 1999.

[4] D. Amit and N. Brunel, "Model of global spontaneous activity and local structured activity during delay periods in the cerebral cortex," *Cerebral Cortex*, vol. 7, pp. 237–252, 1997.

[5] P. Del Giudice, *et al.*, "Modeling the formation of working memory with networks of integrate-and-fire neurons connected by plastic synapses," *Journal of Physiology Paris 97*, pp. 659–681, 2003.

[6] M. Rigotti, *et al.*, "Attractor concretion as a mechanism for the formation of context representations," *NeuroImage*, vol. 52, no. 3, pp. 833–847, 2010.

[7] S. Ganguli, *et al.*, "One-dimensional dynamics of attention and decision making in lip," *Neuron*, vol. 58, no. 1, pp. 15–25, 2008.

[8] G. Gigante, *et al.*, "Bistable perception modeled as competing stochastic integrations at two levels," *PLoS computational biology*, vol. 5, no. 7, p. e1000430, 2009.

[9] J. Braun and M. Mattia, "Attractors and noise: twin drivers of decisions and multistability," *Neuroimage*, vol. 52, no. 3, pp. 740–751, 2010.

[10] X.-J. Wang, "Neural dynamics and circuit mechanisms of decision-making," *Current Opinion in Neurobiology*, 2012.

[11] R. Ratcliff and G. McKoon, "The diffusion decision model: Theory and data for two-choice decision tasks," *Neural computation*, vol. 20, no. 4, pp. 873–922, 2008.

[12] P. Miller and D. B. Katz, "Accuracy and response-time distributions for decision-making: linear perfect integrators versus nonlinear attractor-based neural circuits," *Journal of computational neuroscience*, vol. 35, no. 3, pp. 261–294, 2013.

[13] S. Amari, "Dynamics of pattern formation in lateral-inhibition type neural fields," *Biological Cybernetics*, vol. 27, pp. 77–87, 1977.

[14] J. Hopfield, "Neural networks and physical systems with emergent collective computational abilities," *Proceedings of the national academy of sciences*, vol. 79, no. 8, pp. 2554–2558, 1982.

[15] J. I. Gold and M. N. Shadlen, "The neural basis of decision making," *Annu. Rev. Neurosci.*, vol. 30, pp. 535–574, 2007.

[16] X. Wang, "Probabilistic decision making by slow reverberation in cortical circuits," *Neuron*, vol. 36, no. 5, pp. 955–968, 2002.

[17] K.-F. Wong and X.-J. Wang, "A recurrent network mechanism of time integration in perceptual decisions," *The Journal of neuroscience*, vol. 26, no. 4, pp. 1314–1328, 2006.

[18] S. Moradi and G. Indiveri, "An event-based neural network architecture with an asynchronous programmable synaptic memory," *Biomedical Circuits and Systems, IEEE Transactions on*, vol. 8, no. 1, pp. 98–107, February 2014. [Online].

[19] D. Fasnacht and G. Indiveri, "A PCI based high-fanout AER mapper with 2 GiB RAM look-up table, 0.8 μs latency and 66 M Hz output event-rate," in *Conference on Information Sciences and Systems, CISS 2011*, Johns Hopkins University, March 2011, pp. 1–6.

[20] M. Giulioni, *et al.*, "Robust working memory in an asynchronously spiking neural network realized in neuromorphic VLSI," *Frontiers in Neuroscience*, vol. 5, 2011.

[21] F. Haake, *et al.*, "Passage-time statistics for the decay of unstable equilibrium states," *Physical Review A*, vol. 23, no. 6, p. 3255, 1981.